Atomic Beam Resonance Experiments with Stored Beams*

H. MARK GOLDENBERG,† DANIEL KLEPPNER, AND NORMAN F. RAMSEY
Harvard University, Cambridge, Massachusetts

(Received March 13, 1961)

The atomic-beam separated, oscillatory-field resonance technique has been used to study the hyperfine frequency of cesium which is perturbed by collisions with storage box walls. With a wall coating of long straight-chain saturated hydrocarbons, resonances are observed after as many as 200 wall collisions. A theory of the effect of wall collisions on the hyperfine frequency which is in qualitative agreement with experimental results is described. The shape of the resonance curve is analyzed by a detailed consideration of the statistical nature of the wall collision.

I. INTRODUCTION

THE precision of an atomic beam resonance apparatus is ultimately limited by the transit time of the atoms through the region of interaction with the perturbing fields. For example, in an apparatus using the double oscillatory-field method, the frequency width $\Delta\nu$ of the resonance curve is $0.65\bar{v}/l$ where l is the separation of the rf fields and $\bar{v}$ is the mean velocity in the beam. In order to decrease the resonance width, it is necessary to use slower atoms or to lengthen the distance l. So far, significant improvements by the first method have not been experimentally achieved. Although it is possible to increase l by lengthening the apparatus, the point is soon reached where further increases of length become expensive and inconvenient.

A proposal by Ramsey[1] suggested that the interaction distance might be increased by a large factor without the above difficulties if the atoms were trapped in a storage box between the two rf regions. In this case, the transit time is increased to the mean time an atom spends in the storage box. However, in order for the technique to be successful, it is necessary that collisions with the wall should not significantly perturb the atoms. Preliminary experimental results indicating the existence of a few nondestructive wall collisions have been previously reported.[2] In the following sections, a brief and rather qualitative discussion of the storage-box technique is presented. This is followed by a description of an experimental apparatus constructed to investigate the technique, and a summary of the experimental findings.

II. GENERAL CONSIDERATIONS

An exact theory of wall collisions has not been formulated so far, due to lack of detailed knowledge of surface structure and to the difficulty of carrying out the necessary calculations for even simple two-atom collisions. However, the important features of a wall collision can be understood qualitatively. Some of the characteristics of wall collisions have been analyzed by Babb.[3]

As a first consideration, it is necessary to restrict the choice of atom to be stored to those which are in an S state. States with orbital angular momentum will be relaxed on the surface by Δm_j transitions. Because of this restriction, the following discussion is limited to hyperfine resonance in atoms with an alkali-like electron configuration.

A second, and rather obvious, requirement is that the stored atom should not chemically react with the surface. That is, the adsorption energies must be characteristic of physical adsorption rather than chemical adsorption. Because of this restriction, we can neglect all transition processes which involve excited states of the atoms.

III. INTERACTIONS DURING A WALL COLLISION

A. Nonadiabatic Collisions

The probability that the atom makes a transition to another level of the ground state during a collision is

$$P=[(\mathcal{H}_0/\hbar)\bar{t}_a]^2, \quad (1)$$

where $\mathcal{H}_0$ is the interaction Hamiltonian, and $\bar{t}_a$ is the mean adsorption time. Assuming that there are no unpaired electrons in the surface, we may take, for $\mathcal{H}_0$, the interaction between an electronic and a nuclear dipole moment at a typical adsorption distance of, say, 2 A. The requirement that $P\ll 1$ leads to

$$\bar{t}_a<\hbar\times(2\times10^{-8})^3/10^{-20}\times2\times10^{-23}=4\times10^{-8}\text{ sec}. \quad (2)$$

The adsorption time is related to the adsorption energy E_{ads} by

$$\bar{t}_a=\tau_0\exp(E_{\text{ads}}/kT). \quad (3)$$

τ_0 is the period of vibration of the adsorbed atom in the surface potential well. A reasonable value for τ_0, for a heavy atom, is 10^{-12} sec. Substituting (3) in (2), we have

$$E_{\text{ads}}<kT\ln(4\times10^4)=10kT.$$

This requires that the molar heat of adsorption, at room temperature, is less than 5.5 kcal/mole, which is not a

* This research was supported by the Signal Corps, the National Science Foundation, and the Office of Naval Research.

† National Science Foundation Predoctoral Fellow.

[1] N. F. Ramsey, Rev. Sci. Instr. **28**, 57 (1957).

[2] D. Kleppner, N. F. Ramsey, and P. Fjelstad, Phys. Rev. Letters **1**, 232 (1958).

[3] David Babb, Master's thesis, Massachusetts Institute of Technology, Cambridge, Massachusetts, 1958 (unpublished).

severe restriction for physical adsorption. The adsorbed atom actually migrates over the surface. Since the surface nuclei are randomly oriented, the field the atom experiences is not constant; and consequently, the allowed adsorption energy is even greater than the above estimate indicates.

B. Adiabatic Wall Collisions

The energy levels of the atom are slightly displaced during the collision, providing the collision is not too severe. Since the resonance occurs at the frequency corresponding to the average energy separation, the resonance frequency is correspondingly altered. If the atom undergoes a transition from state p to state q, with energies E_p and E_q, respectively, then a convenient parameter for describing the collision is the phase shift it introduces into the wave function

$$\varphi=\int_{-T}^{+T}\frac{(E_p-E_{p0})-(E_q-E_{q0})}{\hbar}dt. \tag{4}$$

E_{p0} and E_{q0} are unperturbed values of the energies, and the time of integration extends over a single wall collision. If the adsorption time is large compared to the time the atom spends passing through the force field adjacent to the surface, Eq. (4) may be simplified to

$$\varphi=\Delta E\bar{t}_a/\hbar=2\pi\Delta\nu\bar{t}_a, \tag{5}$$

where $\Delta E=(E_{pa}-E_{p0})-(E_{qa}-E_{q0})=\Delta\nu/\hbar$, and $\bar{t}_a$ is the mean adsorption time. E_{pa}, E_{qa} are the average energy levels of the atom while it is adsorbed. The transition frequency of an atom while it is adsorbed is

$$\nu_a=\nu_0+\Delta E/h; \tag{6}$$

ν_0, the free-space resonance frequency is given by

$$\nu_0=(E_{p0}-E_{q0})/h.$$

The observed resonance frequency is $\nu_r=(\bar{E}_p-\bar{E}_q)/h$, where the average is over the time spent between the rf regions. The mean total time spent on the surface is $\bar{n}\bar{t}_a$, where $\bar{n}$ is the mean number of collisions in the box, and the mean time spent in the storage box is $\bar{n}\bar{t}_0$, where $\bar{t}_0$ is the mean time between collisions. Therefore,

$$\nu_r=\nu_0+\Delta\nu\bar{t}_a/\bar{t}_0=\nu_0+\varphi/2\pi\bar{t}_0. \tag{7}$$

It is seen from Eq. (7) that the effect of the wall collisions is to shift the resonance frequency by an amount characteristic of the surface, and proportional to the collision rate, $1/\bar{t}_0$. A discussion of the shape of the resonance line and the effect of relaxation of the wall is given below.

C. Surface Interactions

Upon approaching a surface, an atom is first attracted by induced electrostatic forces, the van der Waals forces. Repulsive forces dominate at separations so small that the charge distributions tend to overlap. These two interactions lead to frequency shifts of opposite sign. The van der Waals interaction lowers the hyperfine interaction by spreading the electron cloud and diminishes the electron density at the nucleus, while the overlap repulsive forces (exchange forces) increase the hyperfine interaction by increasing the electron density at the nucleus. The effects are clearly distinguishable in optical pumping experiments[4,5] and experiments with hydrogen atoms trapped in solid matrices.[6] In optical pumping experiments, if a heavy buffer gas is used, it is found that the average hyperfine interaction decreases, the decrease becoming larger with increasing mass of the buffer gas as expected from the dependence of the van der Waals forces on the atomic polarizability. In a very light buffer gas the repulsive effect predominates and the hyperfine frequency is increased. Because the van der Waals interactions are long range compared to the exchange forces, and because all of the surfaces to be considered are composed of relatively heavy molecules, the effect of the exchange forces is neglected in the following discussion. (A discussion in which both of these effects are considered for the case of an atom colliding with an ideal dielectric surface has been given by Purcell.[7] Adrian[8] discusses both effects for hydrogen trapped in a solid.)

We assume that the adsorption mechanism is due completely to nonpolar van der Waals forces, in which the interaction between two atoms is given by[9]

$$E_W=-\frac{C}{r^6}-\frac{D}{r^8}-\frac{E}{r^{10}}\cdots, \tag{8}$$

where the first term is due to dipole-dipole interaction, the second to dipole-quadrupole interaction, etc. Although all terms but the first are usually neglected, the second term is by no means negligible in the case of a heavy alkali.

Since van der Waals forces are additive, the adsorption energy of an atom on a nonpolar surface may be found by a simple integration. The result is, for the first term in Eq. (8),[10]

$$E_a=-(\pi n/6r_a^3)C, \tag{9}$$

where n is the density of atoms in the solid, and r_a is the adsorption distance.

The constant C depends on the polarizability and

[4] M. Arditti and T. R. Carver, Phys. Rev. **112**, 449 (1958).
[5] L. W. Anderson, F. M. Pipkin, and J. C. Baird, Phys. Rev. Letters **4**, 69 (1960).
[6] C. K. Jen, S. N. Foner, E. L. Cochran, and V. A. Bowers, Phys. Rev. **112**, 1169 (1958); S. N. Foner, E. L. Cochran, V. A. Bowers and C. K. Jen, J. Chem. Phys. **32**, 963 (1960).
[7] E. M. Purcell (private communication).
[8] F. J. Adrian, J. Chem. Phys. **32**, 972 (1960).
[9] J. O. Hirschfelder, C. F. Curtis, and R. B. Bird, *Molecular Theory of Gases and Liquids* (John Wiley & Sons, Inc., New York, 1954).
[10] J. H. deBoer, *Advances in Colloid Science* (Interscience Publishers, Inc., New York, 1950).

excitation energy of the interacting atoms. For the case of an alkali and a nonpolar surface, a convenient expression for C is[11]

$$C=\tfrac{3}{2}\alpha\alpha_s\Delta E\, I/(\Delta E+I), \tag{10}$$

α and α_s are the polarizability of the atom and surface, respectively, ΔE is the difference in energy between the S and P levels in the alkali, and I is the mean ionization energy of the surface. For present purposes, the adsorption distance r_a may be taken as the sum of the kinetic radii of the atom and surface.

The effect of van der Waals forces on the hyperfine energy of an alkali colliding with a rare-gas atom has been considered in detail by Margenau, Fontana, and Klein,[12] and by Herman and Margenau.[12a] In the latter paper it is shown that, to a very good approximation, the shift in hyperfine energy is simply related to the interaction energy in the following fashion:

$$\delta E(\text{hyperfine})=E_W\times h\nu\left(\frac{1}{\Delta E+I}+\frac{2}{I_a}\right), \tag{11}$$

$h\nu$ is the hyperfine separation, I is the mean ionization potential of the rare gas and I_a is the ionization potential of the alkali atom. Adrian[8] shows that the arguments leading to (9) apply to an atom trapped in a solid, and they should also apply to the case of van der Waals adsorption, although the exact value of the ionization potential becomes somewhat ambiguous. From Eqs. (3), (9), and (10) and (11) and (5), we obtain

$$E_a=-\left(\frac{\pi n}{6r_a{}^3}\right)\times\frac{3}{2}\alpha\alpha_s\left(\frac{\Delta E\, I}{\Delta E+I}\right), \tag{12}$$

$$\Delta\nu=\nu_s-\nu_0=\nu_0\times E_a\left(\frac{1}{\Delta E+I}+\frac{2}{I_a}\right), \tag{13}$$

$$\varphi=2\pi\nu_0 t_0\left(\frac{1}{\Delta E+I}+\frac{2}{I_a}\right)E_a\exp(E_a/kT). \tag{14}$$

Equation (14) illustrates the critical dependence of φ on the adsorption parameters. For example, if $E_a=10\,kT$, a 10% change in r_a changes φ by a factor of 3.3. However, Eq. (14) is useful in that it illustrates the desirable features, namely, that the adsorbed atom and surface both have low polarizability. Equation (14) is also useful in comparing the relative merits of different atoms and surfaces, particularly if a value of φ is measured for one combination.

For an order of magnitude estimate of φ, we may use the following values which are appropriate for adsorption of cesium on a hydrocarbon: $r_a=4.4\times10^{-8}$ cm, $n=4\times10^{22}/\text{cm}^3$, $\alpha_s=2.3\times10^{-24}$ cm^3, $\alpha=60\times10^{-24}$ cm^3, $\nu_0=9\times10^9$ cps, $t_0=10^{-12}$ sec, $\Delta E=3.9$ ev, $I=3.5$ ev. The result is $\varphi=1.4\times10^{-1}$ rad/collision.

IV. LINE BROADENING DUE TO SURFACE COLLISIONS

It has been shown above that the resonance frequency is shifted by wall collisions. Because of the random nature of the adsorption process, different atoms are shifted by different amounts. This leads to broadening of the resonance line.

The chief factor in line broadening is the dispersion in adsorption time.[3,13] If $E_a>kT$, then the adsorption time is described by an exponential distribution function: $P(t)=(1/t_a)\exp(-t/t_a)$. This leads to a dispersion in φ given by

$$\delta_1(\varphi)=[\langle\varphi^2\rangle_{\text{av}}-(\langle\varphi\rangle_{\text{av}})^2]^{\frac{1}{2}}=\varphi.$$

After n collisions, the dispersion $\delta_n(\varphi)$ in the accumulated phase shift of the wave function is

$$\delta_n(\varphi)=n^{\frac{1}{2}}\delta_1(\varphi)=n^{\frac{1}{2}}\varphi.$$

For coherence,

$$\delta_n(\varphi)<1 \quad\text{or}\quad n\varphi^2\ll1. \tag{15}$$

A more accurate calculation of the wall relaxation is given in Appendix B where it is shown that the line is broadened by a factor $(1+\frac{1}{2}n\varphi^2)$, and its amplitude is correspondingly decreased.

V. LINE SHAPE

The transition probability P is calculated by a straightforward but lengthy extension of the calculation used in the conventional double oscillatory-field method.[14] The result is summarized in Appendix A. It is shown there that, when the field intensity in each transition region is optimized,

$$P=0.5+0.328\langle\cos\lambda T\rangle_{\text{av}}, \tag{16}$$

where $\lambda=(E_p-E_q)/\hbar$ and T is the time of transit between the two fields. The $\langle\ \rangle_{\text{av}}$ denotes average over time. The averaging process is complicated by the fact that the energy is randomly perturbed by wall collisions so that $\lambda=\lambda(t)$. The shape of the resonance curve for the case of no wall perturbation is described in Sec. A, below. In Sec. B, the case of finite perturbation is discussed.

A. Line Shape with no Wall Perturbations

We assume that the time the atom spends passing between the rf fields but outside the storage box is negligible compared to the mean time in the storage box, which is usually the case. If the geometry of the box is reasonably simple, then the probability that the atom leaves the box instead of making a wall collision is

[11] Reference 9, p. 963.
[12] H. Margenau, P. Fontana, and L. Klein, Phys. Rev. **115**, 87 (1958).
[12a] R. Herman and H. Margenau, Phys. Rev. **122**, 1204 (1961).
[13] P. Fjelstad (private communication).
[14] N. F. Ramsey, *Molecular Beams* (Oxford University Press, New York, 1956).

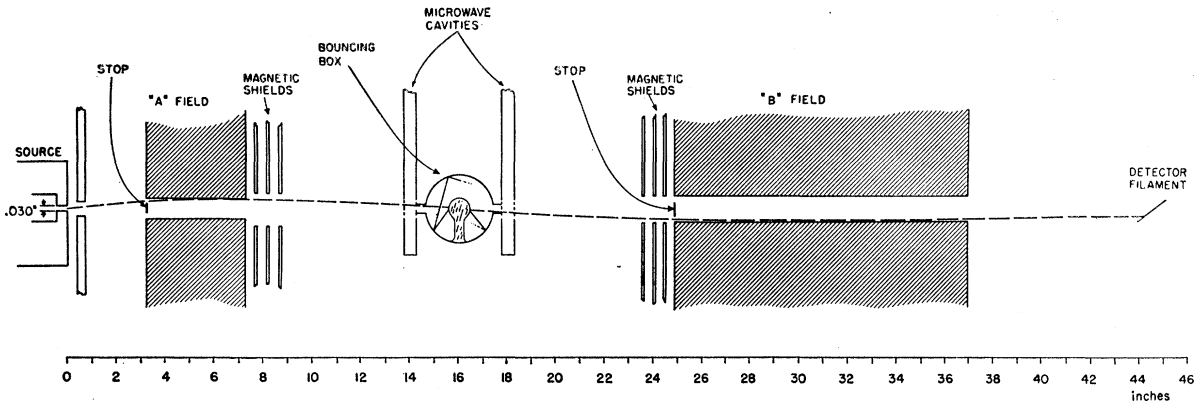

FIG. 1. Schematic diagram of the apparatus.

A_e/A_t, where A_e is the total area of exit from the box and A_t is the total wall area of the box. It follows that the mean number of collisions an atom makes before leaving the box is given by $\bar{n}=A_t/A_e$ and that the distribution function for time spent in the box is

$$P(T)=\gamma \exp(-\gamma T), \tag{17}$$

where $\gamma=1/\bar{n}t_0=1/\bar{t}$. In this case, substituting Eq. (17) into Eq. (16), and carrying out the indicated integration we have

$$P=0.5+0.328\gamma^2/(\gamma^2+\lambda^2). \tag{18}$$

The result is a Lorentzian curve centered about $\lambda=0$, or $(E_{p0}-E_{q0})\nu=h$, with a full width at half-height given by $\Delta\nu_0=\gamma/\pi$.

B. Line Shape with Finite Wall Perturbations

The calculation of $\langle\cos\lambda T\rangle_{\text{av}}$ with finite wall perturbations is outlined in Appendix B. The results are summarized here:

(1) The condition for resonance is

$$\nu=\nu_0+(\tan^{-1}\varphi)/2\pi t_0. \tag{19}$$

(2) The width of the resonance curve is

$$\Delta\nu=\Delta\nu_0(1+\tfrac{1}{2}\bar{n}\varphi^2)$$
$$=\pi^{-1}\gamma(1+\tfrac{1}{2}\varphi^2/t_0). \tag{20}$$

(3) Asymmetries are introduced into the resonance curve if the perturbations are severe, Eq. (B.3). Since this curve cannot be plotted in a reduced form, the amount of asymmetry will not be discussed, except to point out that it is only significant when wall relaxation becomes appreciable, that is when $\frac{1}{2}\bar{n}\varphi^2\approx 1$.

VI. EXPERIMENTAL APPARATUS AND PROCEDURE

A. Choice of Atom

Hydrogen presents itself as a natural choice for storage due to its low polarizability. Early experiments demonstrating specular reflection of H confirm the hypothesis that its adsorption time can be extremely short.[15] Unfortunately, hydrogen has the serious disadvantage of being difficult to detect. This disadvantage becomes prohibitive in the present experiment because of the necessity of recollimating the beam after it leaves the storage box, with a consequent large loss of intensity. Primarily for this reason, it was decided to use Cs^{133} as the working atom. Cesium does have large polarizability, but its experimental convenience made it seem a reasonable choice for a first experiment. The specific transition observed is the $(F=4, m=0)\rightarrow(F=3, m=0)$ hyperfine transition, occurring at 9192 Mc/sec.

B. Apparatus: General Considerations

Because the beam must be recollimated after leaving the storage box there is a very large loss in intensity compared to a conventional apparatus. For this reason, the state selectors are space-focusing hexapolar magnets.[16] The detector, which is described below, has an unusually large ionizing area, and is designed for high collection efficiency.

Preliminary investigation gave irreproducible results which were attributed to surface contamination. For this reason, the present apparatus was designed to be baked out regularly, and a vacuum of about 3×10^{-9} mm Hg can be maintained. Although an adsorbant surface is contaminated in a short time at this pressure, the weakly adsorbing surfaces with which we are primarily concerned do not show any aging or contamination effects.

A schematic diagram of the apparatus is shown in Fig. 1. Atoms effusing from the oven in the $(F=4, m=0)$ state are focused by the "A" magnet and pass through the transition inducing field in the first of the two microwave cavities. The beam passes into the storage box which has a stop between its apertures so that an atom must undergo a number of wall collisions before

[15] F. Knauer and O. Stern, Z. Physik **53**, 799 (1929); T. H. Johnson, J. Franklin Inst. **210**, 145 (1930).

[16] H. Friedburg and W. Paul, Naturwissenschaften **38**, 159 (1951).

effusing out. Those leaving by the second aperture in the correct direction pass through the second microwave cavity and the "B" magnet, and go to the detector. The "B" magnet defocuses atoms in the $(F=3, m=0)$ state, so that the occurrence of resonance causes a decrease in detector signal.

C. Details of the Apparatus

Source

The oven, which is of conventional design, is fabricated from Monel and rests on three sharpened tungsten pins. The well, 1-in. deep by $\frac{1}{2}$-in. diam, is closed at the top by a threaded Monel pressure cap. The source aperture is a 0.030-in. hole and the oven is run at 200–250°C. Cesium metal is doubly distilled and loaded into the well in a glass ampoule under a CO_2 atmosphere. The total flux of Cs atoms in the $(4,0)$ state is about 10^{15} per sec.

Magnets

The "A" magnet has a $\frac{1}{4}$-in. gap diam and is 4-in. long. The maximum field at the pole tip is 7000 gauss, which is achieved with a current of 300 ma flowing through 4250 turns around each pole. The "B" magnet has a $\frac{1}{2}$-in. gap and is 12-in. long. Its maximum field is 6000 gauss, with a current of 400 ma flowing through 3500 turns on each pole. The magnets are mounted externally to the vacuum system, and can be disassembled to allow bakeout. The effective solid angle for atoms in the desired state subtended by each magnet is about 3×10^{-4} steradian.

Detector

The cesium is detected by surface ionization on a hot platinum filament. The filament is $\frac{1}{4}$-in.$\times\frac{3}{4}$-in. by 0.001-in., and is mounted at 45° to the beam axis. The large filament is necessary because the beam leaving the "B" magnet is spread over the magnet-gap area. The ionized cesium is focused at the common center of curvature of a set of four spherical grids which are appropriately biased A small permanent magnet, with a gap strength ot about 2000 gauss, then separates the unwanted potassium background and deflects the beam onto the entrance dynode of a National Company 14-state electron multiplier. The multiplier gain is about 5×10^4 at a supply voltage of 2700 v. The over-all collection efficiency of the detector is about 85%.

The current from the multiplier is amplified in an electrometer and passes to a phase sensitive detector. The output of the detector is displayed by a recorder.

Vacuum System

The vacuum system is fabricated of stainless steel and is pumped by mercury diffusion pumps. With the exception of the rf chamber, which houses the storage box, all demountable joints are sealed with Teflon O-rings. The rf chamber is sealed with aluminum O-rings. A standard bakeout of 200°C overnight results in pressures in the rf chamber which are consistently below 5×10^{-9} mm Hg as measured by an untrapped Veeco ion gauge. Pressures in the non-bakeable detector chamber are below 2×10^{-7} mm Hg, while the source chamber is usually operated at about 5×10^{-7} mm Hg.

Microwave System

The transition regions are tuned X-band microwave cavities. The cavities are independent, and are coupled by a ferrite phase shifter which is used to modulate the resonance by reversing the relative phase in the cavities. The phase is monitored by directional couplers attached to each cavity which drive a common mixer. The separation between the cavities along the beam is 3.5-in. corresponding to a resonance width for an unstored beam of 2 kc/sec.

Frequency generation and stabilization. Because of the relatively narrow resonance line, and the high transition frequency, a stabilized klystron is used as the frequency source. The stabilizing system is illustrated in Fig. 2.

The rf chamber, storage box. The rf chamber houses the two microwave cavities and the storage box between them. The storage box is so mounted that it can be opened in the high vacuum of the rf chamber and can be manipulated in and out of the beam during an experimental run. Heaters on the box support allow heating the box to 150°C.

Figure 3 shows a typical glass storage box. The entrance and exit aperture are $\frac{3}{16}$-in. diam. In the initial phases of these experiments, the glass boxes were baked on a small glass vacuum system at 400°C and then coated with the appropriate material by a triple vacuum distillation and finally sealed under vacuum.

A distillation technique is inapplicable for many of the surfaces investigated, and in such cases other schemes are resorted to. Metallic boxes, and glass boxes with a single wall of a different material have been used, and are described in the next section.

D. Experimental Procedure

After the storage box has been installed and a satisfactory vacuum achieved, the apparatus is tuned

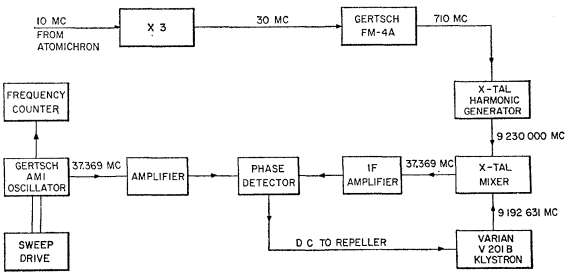

FIG. 2. Frequency stabilizing system.

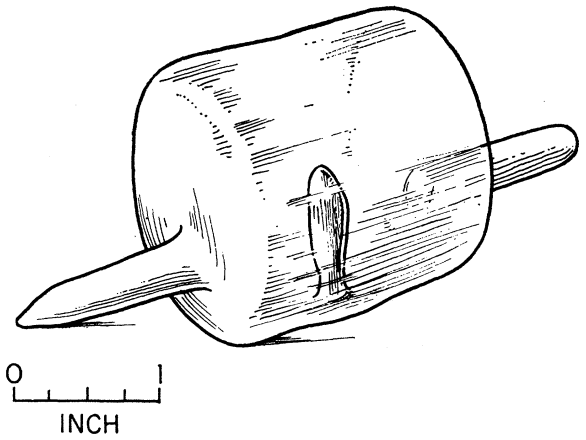

FIG. 3. Typical collision box.

with the storage box out of the beam in order to check the beam intensity and locate the unperturbed hyperfine resonance. The storage box is then raised into the beam. This motion breaks the vacuum seal at the box apertures so that it can admit the beam. A resonance curve is then taken unless the beam has been adsorbed in the box. A typical current from the electron multiplier for the case of a completely nonadsorbing storage box is 1×10^{-8} amp. Under favorable conditions, a signal-to-noise ratio of 40 is obtainable with a one-second integrating time.

Since the apparatus is of the flop-out kind, atoms besides those in the (4,0) state are normally focused. The ratio of total detector current to the modulated component is, therefore, a rough measure of the degree of relaxation. If coherence is preserved, the phase shift per collision is determined from the location of the resonance position and the geometry of the box by means of Eq. (19).

VII. RESULTS

A variety of surface materials were investigated, the majority of which gave complete adsorption or complete relaxation. Of all those tried, only the paraffins allowed a number of collisions large enough to yield quantitative information on the phase shift. The results for the paraffins are summarized below, and are followed by a brief summary of findings for other surfaces investigated.

A. Paraffin

The most reliable surface material investigated was "Paraflint" (Moore and Munger, New York), which is the trade name for a mixture of long chain paraffins of the type $CH_3(CH_2)_nCH_3$, where n varies between 40 and 60. The melting temperature is between 103° and 108°C. Fractional distillation revealed that the lightest components melt at 77°–79°C, while the heaviest melt at 118°–120°C.

Data were obtained using a number of different storage boxes with $\bar{n}$ varying between 60 and 190. The mean phase shift per collision was determined to be

$$\varphi=0.09\pm0.01 \text{ rad/collision.}$$

If we substitute this value in Eq. (14), and assume that $I=6.4$ ev, we obtain $E_a=0.8$ ev$=1.9$ kcal/mole.

The recorder trace of the resonance in a storage box with $\bar{n}=60$ is shown in Fig. 4. The mean time between collisions $\bar{t}_0=6.7\times10^{-5}$ sec. The unperturbed linewidth for this box would be $\Delta\nu=80$ cps. The resonance frequency is displaced -225 cps, and the measured linewidth is 150 cps. Using (20), we find that the predicted linewidth is 100 cps, which is in qualitative agreement with the observed linewidth. Linewidths as narrow as 80 cps in a box with $\bar{n}=200$ have been recorded. However, this is in the region of very strong relaxation ($\bar{n}\varphi^2/2=0.8$) and the signal-to-noise ratio is consequently poor.

The best results were obtained with the box heated slightly above the melting point of the paraffin, so that the atoms were actually adsorbed on a liquid surface. No appreciable difference was observed with surfaces composed of distilled fractions of the "Paraflint." Dotriacontane $[CH_3(CH_2)_{30}CH_3]$ and tetracontane $[CH_3(CH_2)_{40}CH_3]$ were also tried, and yielded slightly larger phase shifts than "Paraflint."

B. Other Surfaces

Halogenated paraffin. "Halocarbon" Wax (Halocarbon Products Corporation). This is a fully halogenated chlorofluorocarbon wax. It completely adsorbed the beam, most probably due to chemical reaction with the halogens.

Teflon. Earliest results were obtained with a Teflon surface.[2] However, attempts to store beams for more than a few collisions failed due to chemical adsorption of the beam. The beam intensity can be explained by assuming that there is a probability of 0.1 that an atom sticks to the surface on a given collision. Those atoms which did leave the box still displayed a resonance, and though it was impossible to obtain long enough storage times to measure φ, it can be concluded from the lack

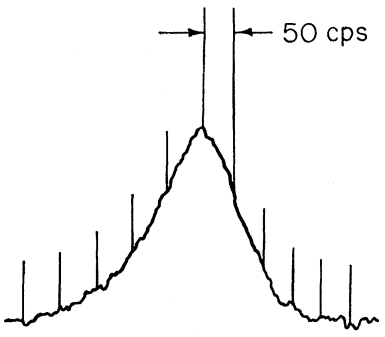

FIG. 4. Resonance curve for "Paraflint."

of relaxation that $\varphi<1$, in spite of chemical adsorption taking place.

Meltable polyethylene. A sample of "Nieder-Moleculares Polyättylën" which has a melting point of about 100°C was studied in a box with $\bar{n}=65$. The cesium beam was completely adsorbed. It is likely that this material contained catalytic impurities and cracked chains, both of which would react chemically with cesium.

High-purity polyethylene A variety of polyethylenes with low dielectric loss were studied. These gave irreproducible results due to the difficulty of preparing a clean undamaged surface. However, the best results compared favorably with those of paraffin.

Dichlorodimethylsilane (General Electric "Dri Film"). Our interest in this substance was due to its use in inhibiting surface recombination of atomic hydrogen.[17] However, four separate runs indicated complete surface relaxation, although there was no appreciable adsorption.

LiF. A freshly cleaved LiF surface was mounted on a $\frac{1}{2}$-in. diam hole bored in a 2-in. diam glass storage box which was covered with "Paraflint." The cleaved LiF surface completely adsorbed the beam.

Sapphire. A setup similar to that used for LiF was used, and the result was complete adsorption.

Glass. Glass was run as a testing measure to ensure that a known adsorbing surface actually behaved as such under typical experimental conditions. There was complete adsorption to 150°C.

SiO_2. A fused quartz storage box was mounted in a special oven which could be heated to 750°C. The beam was completely adsorbed at room temperature, as expected. As the temperature was raised to about 500° the cesium beam began to reappear but no resonance was obtainable. At 750°, the adsorption time was still in the order of seconds, and the beam was completely relaxed.

Nickel. Cesium should relax on collision by spin exchange even in the absence of chemical adsorption. It has been reported[18] that the condensation coefficient of cesium on nickel is 0. A 0.001-in. nickel coating was electrolytically applied to an aluminum box with $\bar{n}=190$. The beam was completely adsorbed at temperatures up to 150°C.

Pyrolytic graphite. ("Pyrographite," supplied by Raytheon Company). Pyrolytic graphite is graphite in a highly oriented state which is composed of practically perfect planes. The planar surface has very weak adsorptive properties, and a preliminary test with a small sample covering an opening in a paraffin-covered bulb showed that it did not appreciably adsorb the beam or perturb the resonance. However, a storage box fabricated entirely from pyrolytic graphite showed complete adsorption. Unfortunately, the sample from which the box was fabricated had been machined, which may have destroyed the orientation of the surface. Since no other samples were available, the results are inconclusive.

VIII. CONCLUSION

The most favorable substance found for the storage box allowed observation of resonances with approximately 200 wall collisions but perturbed the resonance too much to allow high precision spectroscopy. However, the search has not been unfruitful, for the limited success with paraffin walls allows one to make predictions about the use of the technique with other atoms. For instance, hydrogen has a much smaller polarizability than cesium (0.8×10^{-24} cm^3 compared to about 60×10^{-24} cm^3 for cesium). τ_0, the period of vibration of an adsorbed atom in the surface potential well, varies with the square root of the mass, and is therefore smaller by a factor of about 12 for hydrogen. Therefore, from Eqs. (12) and (14) we see that the phase shift for hydrogen should be considerably smaller than for cesium. Since the maximum number of useful collisions varies inversely as the square of φ, it is realistic to expect that hydrogen can be stored for much longer storage times with the number of wall collisions vastly greater than the 200 possible with cesium. With long enough storage times, maser action can be used to detect the resonance, rather than a conventional beam detector, thereby eliminating the initial objection to hydrogen. This has proven to be feasible. The successful use of the storage-box technique in an atomic-hydrogen maser has been reported elsewhere.[19]

ACKNOWLEDGMENTS

We wish to acknowledge the contribution of Paul Fjelstad in some of the first experiments, in analyzing the effect of surface relaxation, and in calculating the line shapes. Conservations with Carroll Alley on the use of buffer walls have been most helpful, and we would particularly like to thank him for suggesting the use of "Paraflint."

APPENDIX A

Transition Probability for a Stored Atomic Beam

The transition probability for an atomic beam resonance using the double oscillatory-field method has been worked out by Ramsey,[14] and we will use his notation.

The atom is initially in state p. It is desired to find the probability P that the atom has made a transition to state q after traversing two oscillatory fields in which transitions are induced by perturbations of the form $V_{p,q}=\hbar b\exp(i\omega t)$. Let subscript 1 refer to quantities in the first field, and subscript 2 refer to quantities in the second field. The flight of the atom is interrupted by a

[17] J. P. Wittke and R. H. Dicke, Phys. Rev. **103**, 620 (1956).
[18] S. Wexler, Revs. Modern Phys. **30**, 402 (1958).
[19] H. M. Goldenberg, D. Kleppner, and N. F. Ramsey, Phys. Rev. Letters **5**, 361 (1960).

storage box placed midway between the fields. We use the following notation: t=time in rf field, T=time spent in the storage box, ω_0=resonant frequency, $a=[(\omega-\omega_0)^2+(2b)^2]^{\frac{1}{2}}$, l=length of rf field, L=distance from either field to storage box, $\lambda=\omega_0-\omega$, $x=2b/\alpha$, $x^{\pm}=(2b\pm\lambda L)/\alpha$, α=most probable velocity of atom. The following function is of use, and is tabulated in reference 14, p. 425:

$$I(x)+iK(x)=\int_0^\infty \exp[-y^2+i(x/y)]dy.$$

The following expression is obtained for P for the case when $|\omega-\omega_0|\ll 2b$:

$$\begin{aligned}P=&\tfrac{1}{2}-2I(x_1)I(x_2)\\&+\tfrac{1}{2}\cos\lambda T\{[K(x_1^+)+K(x_1^-)][K(x_2^+)+K(x_2^-)]\\&-[I(x_1^+)-I(x_1^-)][I(x_2^+)-I(x_2^-)]\\&-\tfrac{1}{2}\sin\lambda T\{[K(x_1^+)+K(x_1^-)][I(x_2^-)-I(x_2^+)]\\&+[I(x_1^-)-I(x_1^+)][K(x_2^+)+K(x_2^-)]\}.\end{aligned}$$

P is maximum when

$$2b_1l_1/\alpha_1=2b_2l_2/\alpha_2=0.600\pi.$$

In this case, and when $L/\alpha\ll\bar{T}$, the above expression reduces, when averaged over time, to

$$P=0.5+0.328\langle\cos(\lambda T)\rangle_{\rm av},$$

which is the equation given in the text.

APPENDIX B

Shape of the Resonance Line

It is desired to evaluate $\langle\cos\lambda T\rangle_{\rm av}$. We will make use of the following relations: $n-1$=number of collisions an atom makes before leaving, t_0=mean time between collisions, τ=total time an atom is adsorbed, T=time an atom spends in the box=nt_0. Using notation similar to that of Sec. III B,

$$\lambda=(\omega-\omega_r)=\omega-\omega_0-\Delta\omega\tau/T=\lambda_0-\Delta\omega\tau/T.$$

The following distribution functions are involved: (1) Distribution in number of collisions made by an emerging atom

$$p(n)=\delta(1-\delta)^n,$$

δ=probability of leaving per collision. (2) Distribution in total time spent on surface after n collisions; it is stated in the text that the distribution in adsorption time is given by

$$F_1(\tau)=(1/\bar{t}_a)\exp(-\tau/\bar{t}_a),$$

where t_a is the mean adsorption time. From this it follows that the distribution in total time spent on the surface after n collisions is given by

$$F_n(\tau)=\frac{\tau^{n-1}}{(n-1)!\bar{t}_a{}^n}\exp(-\tau/\bar{t}_a).$$

Neglecting for the moment the distribution in t_0, we have

$$\begin{aligned}&\langle\cos\lambda T\rangle_{\rm av}\\&=\langle\cos\{(\lambda_0-\omega_a\tau/T)T\}\rangle_{\rm av}=\langle\cos(\lambda_0T-\omega_a\tau)\rangle_{\rm av}\\&=\sum_{n=1}^{\infty}\delta(1-\delta)^{n-1}\int_0^\infty F_n(\tau)\cos(n\lambda_0t_0-\omega_a\tau)d\tau \qquad (B.1)\\&=\frac{A\cos\theta-B}{\bar{n}(A^2+B^2-2AB\cos\theta)}, \qquad (B.2)\end{aligned}$$

where $A=(1+\varphi^2)^{\frac{1}{2}}$, $B=1-1/\bar{n}$, $\theta=\lambda_0t_0-\tan^{-1}\varphi$, $\varphi=\Delta\omega\tau_0$, and $\bar{n}=1/\delta$. The resonant condition is now

$$\lambda_0t_0=\tan^{-1}\varphi,$$

or

$$\nu=\nu_0+\tan^{-1}\varphi/2\pi t_0.$$

The width of the curve at half-height is approximately

$$\Delta\nu=\frac{1}{\pi}\left(\frac{1}{\bar{n}t_0}+\frac{\varphi^2}{2t_0}\right)=\Delta\nu_0(1+\tfrac{1}{2}\bar{n}\varphi^2).$$

Equation (B.2) is symmetric about the resonant frequency. However, if we alter Eq. (B.1) to include a distribution over t_0, using the following normal distribution function:

$$\begin{aligned}P(t)&=(2/\pi\sigma^2)^{\frac{1}{2}}\exp[-(t-t_0)^2/2\sigma^2],\\P(t=nt_0)&=(2/n\pi\sigma^2)^{\frac{1}{2}}\exp[-(t-nt_0)^2/2n\sigma^2],\end{aligned}$$

we obtain

$$\langle\cos\lambda T\rangle_{\rm av}=\frac{AC\cos\theta-B}{\bar{n}(A^2C+B^2-2AB\cos\theta)}, \qquad (B.3)$$

where $C=\exp(\lambda_0^2\sigma^2)$. Typically, $\sigma\approx t_0$. Equation (B.3) is no longer symmetric about the frequency of maximum transition probability.